Hydroformylation of alkenes using heterogeneous catalyst prepared by intercalation of HRh(CO)(TPPTS)$_3$ complex in hydrotalcite

Sumeet K. Sharma [a,b], Parimal A. Parikh [b], Raksh V. Jasra [a,*]

[a] Discipline of Inorganic Materials & Catalysis, Central Salt and Marine Chemicals Research Institute (CSMCRI), G.B. Marg, Bhavnagar 364 002, Gujarat, India
[b] Department of Chemical Engineering, SV National Institute of Technology, Surat 395 007, Gujarat, India

ABSTRACT

Intercalation of HRh(CO)(TPPTS)$_3$ complex into the interlayer space of hydrotalcite was carried out to prepare an eco-friendly heterogeneous hydroformylation catalyst. Intercalated catalyst was characterized by ^{31}P NMR, P-XRD, FT-IR, SEM and surface area measurements. Catalytic activity of intercalated catalyst [HT(3.5)-INT] was evaluated for hydroformylation of linear alkenes of varied carbon number from C$_5$ to C$_{13}$ as well as cyclic alkenes. Selectivity of the aldehydes was observed to decrease with increase in the carbon chain length of linear alkenes. Effect of reaction parameters on catalytic activity of intercalated catalyst was studied by varying the catalyst amount, 1-hexene concentration, reaction temperature, partial pressure of carbon monoxide and hydrogen for hydroformylation of 1-hexene. The catalyst was re-cycled up to five times without significant loss in the alkene conversion and selectivity of aldehydes.

1. Introduction

Hydroformylation or oxo reaction employed for the synthesis of aldehyde and alcohol starting from alkene is an important reaction from industrial and academic perspective. Approximately, 9 million metric tons per year of aldehydes and alcohols are produced using hydroformylation reaction. These products find applications in the manufacturing of soaps, fragrances, detergents, adhesives, plasticizers and solvents [1–3]. Commercially, triphenylphosphine modified rhodium based complex is used as a catalyst for hydroformylation of lower carbon chain alkenes (C$_2$–C$_5$) under milder reaction conditions. However, this is not used for higher carbon chain length alkenes due to the decomposition of rhodium complex during separation of catalyst from product mixture. This problem is solved by using water soluble, [HRh(CO)(TPPTS)$_3$] catalyst in biphasic system for the hydroformylation [4]. The application of biphasic catalyst system is limited to hydroformylation of propylene and butene due to lower solubility of higher carbon chain length alkenes in aqueous medium. Hydroformylation of higher alkenes is carried out using cobalt based catalysts under homogeneous conditions. These catalysts require higher temperature, pressure and longer reaction time as compared to rhodium based catalysts.

Selectivity of aldehyde is low in case of cobalt catalyzed hydroformylation of alkenes. Though, homogeneous catalysts give higher conversion and selectivity for desired product in shorter reaction time as compared to heterogeneous catalyst system, yet have disadvantage in the separation of catalyst from product mixture. Thus, research efforts are directed towards the heterogenization of rhodium complex for hydroformylation of alkenes. Therefore, numerous supported rhodium complexes have been reported in the literature for the hydroformylation of alkenes. The support materials studied include MCM-41, silica, alumina, zeolites, activated carbons, polymeric organic, inorganic and hybrid supports, supported aqueous phase catalysis (SAPC) [5–14a]. Main disadvantages of these supported catalysts are, leaching of rhodium complex during the reaction, complicated synthesis procedure, lower catalyst activity and thermal instability. Application of fluorous solvents for biphasic hydroformylation of alkenes is also reported in literature to separate the catalyst from product mixture [14b].

Hydrotalcite or layered double hydroxides (LDHs), are synthetic anionic clays having positively charged brucite-like sheets with general formula $[M(II)_{1-x}M(III)x(OH)_2]^{x+}A^{n-}{}_{x/n}(1-3x/2)H_2O$ (0.20 < x ≤ 0.33), where M(II) and M(III) are divalent and trivalent cations in the octahedral sites within the hydroxyl layers, x is the molar ratio of M(III)/[M(II) + M(III)] and A is the exchangeable interlayer anions [15]. Due to excellent anion exchange property of hydrotalcite, variety of organic and inorganic anions can be intercalated into the interlayer space of hydrotalcite and obtained material can be used for specific application [16–27]. Intercalation of transition metal complexes such as PtCl$_6$,

* Corresponding author. Present address: R&D Centre, VMD, Reliance Industries Limited, Vadodara, 391 346, Gujarat, India. Tel.: +91 265 6696313; fax: +91 265 6693934.
E-mail address: rakshvir.jasra@ril.com (R.V. Jasra).
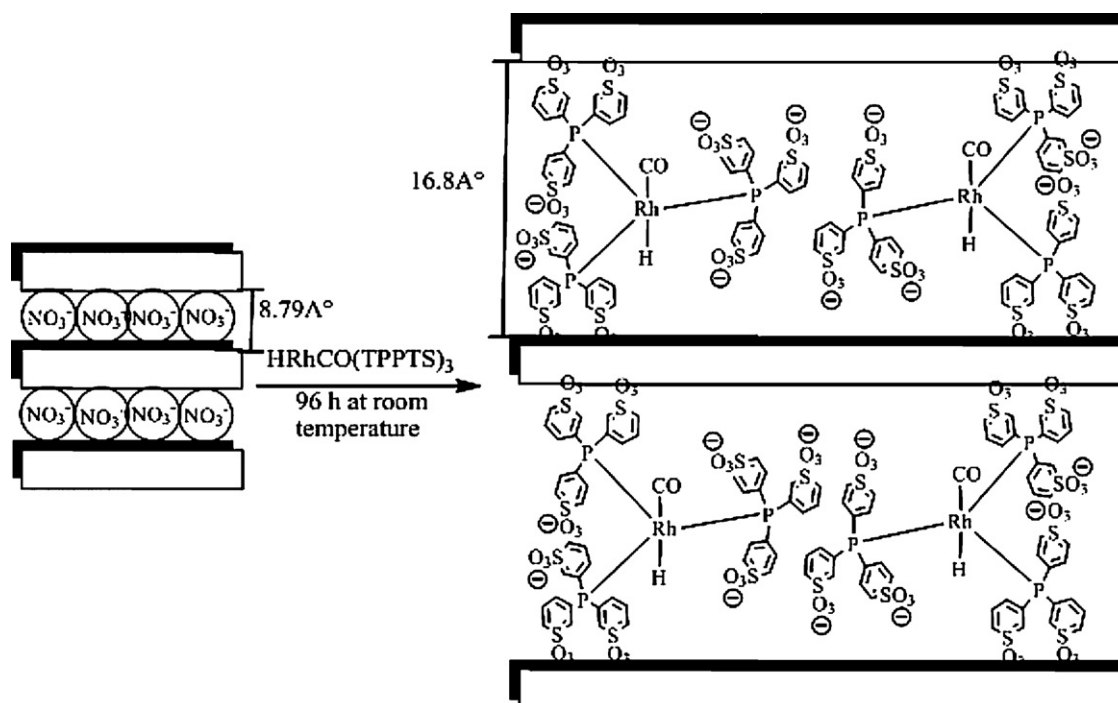
Scheme 1. Intercalation of HRh(CO)(TPPTS)$_3$ complex into the interlayer space of hydrotalcite.

palladium, cobalt(II)-phthalocyanine, ruthenium-, chromium-, iron(III)-hexacyano, copper(II)- and nickel(II)-nitrilotriacetate in the layered double hydroxide has been reported in the literature [28–37]. Intercalation of trans-RhCl(CO)(TPPTS)$_2$ complex with and without excess TPPTS [tris(m-sulfonatophenyl)phosphine] into Zn–Al layered double hydroxides was reported by Duan et al., and trans-RhCl(CO)(TPPTS)$_2$ complex intercalated with excess TPPTS was used as a catalyst for hydroformylation reaction [38]. In another study, RhCl(TPPTS)$_3$ complex was heterogenized onto Zn–Al layered double hydroxides via ion exchange method and used as a heterogeneous catalyst for hydrogenation of bicyclo[2.2.2]octenes [39]. In the present study, intercalation of HRh(CO)(TPPTS)$_3$ complex was carried out in the interlayer space of Mg–Al hydrotalcite of Mg/Al molar ratio of 3.5 (Scheme 1) and applicability of intercalated complex as a heterogeneous catalyst for hydroformylation of alkenes was studied in detail.

2. Experimental

2.1. Materials

The (acetylacetonato)dicarbonylrhodium (Rh(CO)$_2$(acac); 98%), tris(3-sodium sulfonatophenyl) phosphine (TPPTS; P(m-C$_6$H$_4$SO$_3$Na)$_3$), and alkenes were purchased from Sigma–Aldrich, USA. Magnesium nitrate (Mg(NO$_3$)$_2$·6H$_2$O, 99.99%), aluminum nitrate (Al(NO$_3$)$_3$·9H$_2$O, 99.99%), sodium nitrate (NaNO$_3$, 99.99%), ammonia solution (40%) and toluene (99.9%) were purchased from s.d. Fine Chemicals, India. CO (99.9%) and H$_2$ (99.99%) gases were purchased from Alchemie Gases and Chemicals Pvt. Ltd., India. Double distilled milli-pore deionized water was used during the synthesis of catalyst.

2.2. Synthesis of HRh(CO)(TPPTS)$_3$ complex

Synthesis of HRh(CO)(TPPTS)$_3$ complex was carried out by reported procedure [40]. In a typical procedure, 400 mg of TPPTS

(0.704 mmol) was dissolved in 1 mL water followed by addition of 50 mg of Rh(CO)$_2$(acac) under inert atmosphere. Mixture was warmed gently till the complete dissolution of Rh(CO)$_2$(acac). Syngas (CO + H$_2$ = 1:1) was charged into solution from top of the flask. Color of the solution changed from maroon to yellow on passing syn-gas. After 6 h, solution was filtered to remove unreacted rhodium metal under inert atmosphere. Yellow precipitate was obtained by adding saturated ethanol (8 mL) with syn-gas into the filtrate. The precipitated material was again filtered, washed with ethanol and dried under vacuum.

2.3. Synthesis of hydrotalcite [HT(3.5)-N]

Hydrotalcite of Mg/Al molar ratio 3.5 [HT(3.5)-N] was synthesized by co-precipitation of metals salt solutions at constant pH [15]. Typically, for synthesis of hydrotalcite of Mg/Al molar ratio 3.5, an aqueous solution (A) of Mg(NO$_3$)$_2$·6H$_2$O (0.105 mol) and Al(NO$_3$)$_3$·9H$_2$O (0.03 mol) in 80 mL double distilled deionized water was prepared. The solution A was added drop wise into a second solution (B) containing NaNO$_3$ (0.10 mol) in 80 mL double distilled deionized water, for about 1 h under vigorous stirring at room temperature. pH of the content was maintained to 9.5 by adding the ammonia solution. The content was aged at 65 °C for 14 h under autogenous pressure. The formed precipitate was filtered and washed with hot distilled water until pH of filtrate was 7. Washed precipitate was dried in vacuum at room temperature.

2.4. Intercalation of HRh(CO)(TPPTS)$_3$ complex into the layers of hydrotalcite[HT(3.5)-INT]

Intercalation of HRh(CO)(TPPTS)$_3$ complex into interlayer space of [HT(3.5)-N] was carried out by addition of 3.24 g hydrotalcite in a solution of 1.04 g HRh(CO)(TPPTS)$_3$ complex in 25 mL deionized double distilled water. The suspension was stirred at room temperature for 96 h under inert atmosphere of nitrogen gas. After 96 h, yellow color suspension was filtered and dried in vacuum and the catalyst thus obtained was termed as [HT(3.5)-INT].
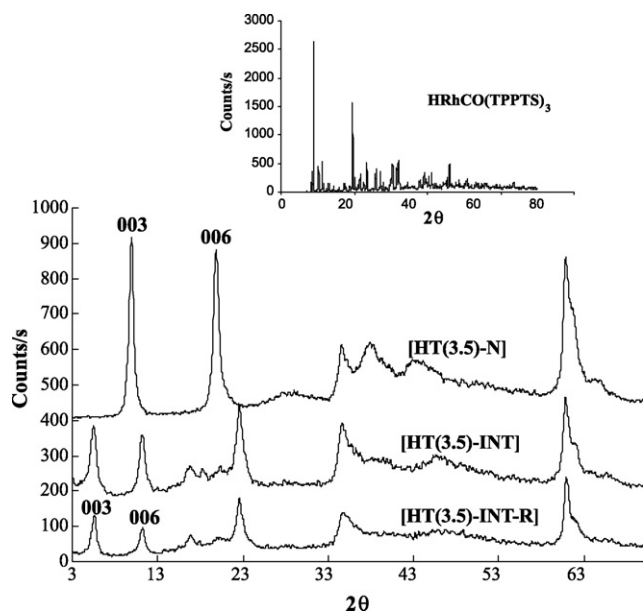
Fig. 1. P-XRD patterns of HRh(CO)(TPPTS)₃ complex, [HT(3.5)-N], [HT(3.5)-INT] and [HT(3.5)-INT-R] catalysts.

2.5. Characterization of catalyst

Powder X-ray diffraction (P-XRD) patterns of HRh(CO)(TPPTS)₃ complex, [HT(3.5)-N] and [HT(3.5)-INT] were recorded using Phillips X'Pert MPD system equipped with XRK 900 reaction chamber, using Ni-filtered Cu Kα radiation ($\lambda = 1.5405$ Å) over a 2θ range of 2–70°. Percentage crystallinity of [HT(3.5)-N] and [HT(3.5)-INT] was calculated by the summation of integral intensities of (0 0 3) and (0 0 6) planes and compared with pristine hydrotalcite [HT(3.5)-N]. Values of unit cell parameters (a and c) of [HT(3.5)-N] and [HT(3.5)-INT] were calculated by the formula; $a = 2(d_{110})$ and $c = 3(d_{003})$; where d_{110} and d_{003} are the basal spacing values of (1 1 0) and (0 0 3) planes, respectively [41].

Fourier transform infrared spectra (FT-IR) of HRh(CO)(TPPTS)₃ complex, [HT(3.5)-N] and [HT(3.5)-INT] were recorded using PerkinElmer spectrum GX FT-IR system in the region of 400–4000 cm⁻¹ using KBr pellets.

³¹P MAS NMR spectra of TPPTS, HRh(CO)(TPPTS)₃ complex and [HT(3.5)-INT] were recorded on Bruker Avance II-500 (FT-NMR–500 MHz) spectrometer.

Thermogravimetric analysis (TGA) of HRh(CO)(TPPTS)₃ complex, [HT(3.5)-N] and [HT(3.5)-INT] was carried out using Mettler TGA/SDTA 851e equipment in flowing nitrogen (flow rate = 50 mL/min), at a heating rate of 10 °C/min.

Surface morphology of the [HT(3.5)-N] and [HT(3.5)-INT] was determined using scanning electron microscope (Leo Series VP1430, Germany) having silicon detector. The samples were coated with gold using sputter coating prior to measurement. Analysis of samples was carried out at an accelerating voltage of 15 kV. Chemical analysis of the catalyst was carried out using Inductive Coupled Plasma (ICP) Spectrometer, PerkinElmer, Optima 2000 instrument.

Surface area measurements of [HT(3.5)-N] and [HT(3.5)-INT] were carried out using ASAP 2010 Micromeritics, USA. Samples were activated at 80 °C for 4 h under vacuum (5×10^{-2} mmHg) prior to N₂ adsorption measurements. Specific surface area of the

samples was calculated from N₂ adsorption isotherms measured at 77.4 K using Brunauer, Emmett, Teller (BET) method. Pore size distribution was calculated from desorption branch using the Barrett, Joyner and Halenda method [42].

2.6. Hydroformylation reaction

Hydroformylation reaction was carried out in 100 mL EZE–Seal stirred reactor supplied by Autoclave Engineers, USA, equipped with a controlling unit [43,44]. In a typical reaction procedure, 0.025 moles of 1-hexene and 0.1 g tridecane (as an internal standard) dissolved in 50 mL of toluene as a solvent with 100 mg of [HT(3.5)-INT] catalyst were added into the reactor. The reactor was flushed twice with nitrogen after that the synthesis gas (CO/H₂ = 1:1) was introduced into the reactor up to 40 atm. The reactor temperature was brought up to 80 °C by heating and stirrer of the reactor was started at 1000 rpm. Constant pressure was maintained during the reaction by supplying syn-gas from reservoir. After completion of the reaction, reactor was cooled to room temperature by circulation of cold water in the coil provided inside the reactor. Product mixture was then analyzed by gas chromatography (GC) and GC–mass spectroscopy (GC–MS).

For finding out reusability, the catalyst was filtered from reaction mixture, washed with 100 mL toluene and dried in vacuum. The catalyst obtained after drying was used for hydroformylation of 1–hexene under reaction conditions similar to that of fresh catalyst.

2.7. Reaction product analysis

Analysis of product mixture was carried out by GC–MS (Shimadzu, GCMS–QP2010) and GC (Shimadzu 17A, Japan) equipped with 5% diphenyl and 95% dimethyl siloxane universal capillary column (60 m length and 0.25 mm diameter) and a flame ionization detector (FID). GC oven temperature was programmed from 40 to 200 °C at the rate of 6 °C/min. Nitrogen gas was used as a carrier gas. Temperatures of injection port and FID were kept constant at 200 °C. Retention times of different compounds were determined by injecting pure compound under identical conditions. To ensure reproducibility of the reaction, repeated experiments were carried out under identical reaction conditions. The conversion and selectivity data was found to be reproducible in the range of ±3% variation. % conversion of alkenes, % selectivity of aldehydes and TOF values were calculated by following formula:

$$\% \, \text{Conversion} = \frac{\text{Moles of alkene reacted}}{\text{Moles of alkene fed}} \times 100$$

$$\% \, \text{Selectivity of aldehydes} = \frac{\text{Moles of aldehydes formed}}{\text{Moles of (aldehydes + isomerized alkene + alkane)}} \times 100$$

$$\text{TOF} = \frac{\text{Moles of aldehydes formed}}{(\text{Moles of Rh present in the catalyst} \times \text{time})}$$

3. Results and discussion

3.1. Characterization of catalyst

P-XRD patterns of HRh(CO)(TPPTS)₃, [HT(3.5)-N] and [HT(3.5)-INT] are shown in Fig. 1. P-XRD pattern of [HT(3.5)-N] shows sharp and symmetric peaks at lower diffraction angles ($2\theta = 10$–25) and broad asymmetric reflections at higher angles ($2\theta = 30$–50), which are typical characteristics of pure hydrotalcite. The presence of NO₃⁻ anions in interlayer space of [HT(3.5)-N] was confirmed by the d-spacing of (0 0 3) and (0 0 6) planes, 8.79 and 4.48 Å, respectively. P-XRD pattern of intercalated material [HT(3.5)-INT] shows all characteristics peaks of pristine hydrotalcite without

any additional peak of HRh(CO)(TPPTS)$_3$ complex. This indicates intercalation of complex into the interlayer space of [HT(3.5)-N]. However, in our earlier work for the synthesis of multi-functional catalyst system by impregnation of HRh(CO)(PPh$_3$)$_3$ complex on the surface of hydrotalcite, we have observed the peaks of HRh(CO)(PPh$_3$)$_3$ complex in the P-XRD pattern of multi-functional catalyst [45,46]. The main diffraction peaks at 2θ values 5.62 (0 0 3), 11.32 (0 0 6) and 61.1 (1 1 0) were observed in P-XRD pattern of [HT(3.5)-INT] sample. The observed shift in P-XRD pattern of intercalated [HT(3.5)-INT] sample towards lower 2θ values of (0 0 3) and (0 0 6) planes with respect to pristine hydrotalcite confirmed the intercalation of HRh(CO)(TPPTS)$_3$ complex. The intercalation of HRh(CO)(TPPTS)$_3$ complex was further confirmed by the broadening in d-spacing value of (0 0 3) plane of [HT(3.5)-INT] from 8.79 to 16.8 Å. In order to observe the effect of intercalation of HRhCO(TPPTS)$_3$ complex on the crystallinity of hydrotalcite [HT(3.5)-N], the pristine hydrotalcite was considered as a 100% crystalline sample. The crystallinity of [HT(3.5)-INT] was observed to decrease up to 43% on intercalation of HRh(CO)(TPPTS)$_3$. The values of unit cell parameters a were calculated as 3.0 Å for both, [HT(3.5)-N] and [HT(3.5)-INT]. The value of c was observed to change significantly for intercalated sample [HT(3.5)-INT]. The value of c was calculated as 26.4 Å for [HT(3.5)-N], which increased to 59.4 Å for [HT(3.5)-INT]. The increase in the c value for [HT(3.5)-INT] catalyst is due to the broadening d-spacing of (0 0 3) plane by intercalation of HRh(CO)(TPPTS)$_3$ complex in the [HT(3.5)-N].

FT-IR spectra of HRh(CO)(TPPTS)$_3$, [HT(3.5)-N] and [HT(3.5)-INT] are shown in Fig. 2. Formation of HRh(CO)(TPPTS)$_3$ complex
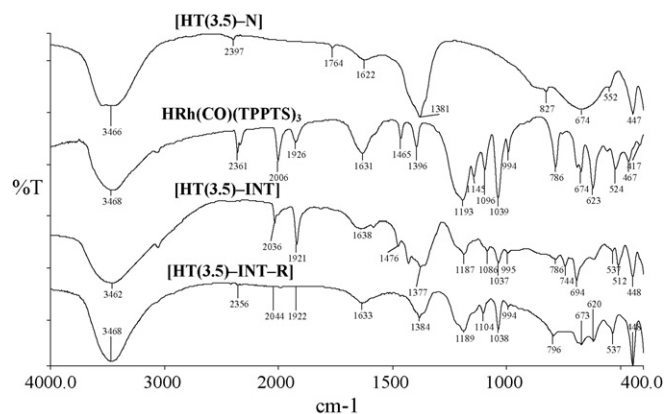
Fig. 2. FT-IR spectra of [HT(3.5)-N], HRh(CO)(TPPTS)$_3$ complex, [HT(3.5)-INT] and [HT(3.5)-INT-R] catalysts.

was confirmed by the appearance of bands at 2006 cm^{-1} for ν_{Rh-H}, 1926 cm^{-1} for $\nu_{C=O}$, 3468 and 1631 cm^{-1} for ν_{O-H}, 1465 and 1396 cm^{-1} for ν_{ph}, 1193 cm^{-1} for ν_{SO3^-}, 1096 cm^{-1} for ν_{SO} and 623 cm^{-1} for ν'_{SO} [38]. The band appeared at 1381 cm^{-1} in FT-IR spectrum of [HT(3.5)-N] confirms the presence of nitrate anions in the interlayer space of hydrotalcite [15]. The bands at 1193 cm^{-1}(ν_{SO3^-}), 1096 cm^{-1}(ν_{SO}) and 623 cm^{-1} (ν'_{SO}) in the spectrum of HRh(CO)(TPPTS)$_3$ complex was observed to shift towards low frequency region in the FT-IR spectrum of [HT(3.5)-INT] cat-
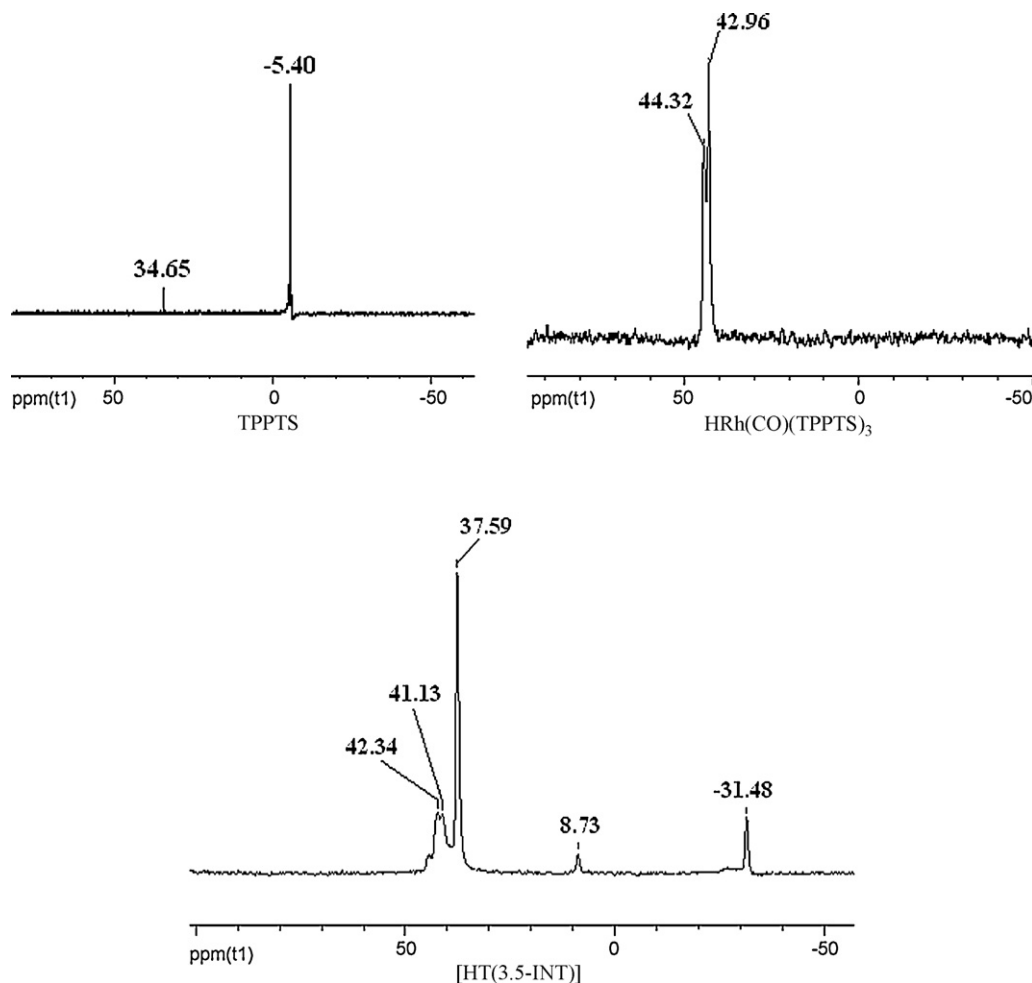

Fig. 3. ^{31}P NMR spectra of TPPTS, HRh(CO)(TPPTS)$_3$ complex and [HT(3.5)-INT] catalysts.
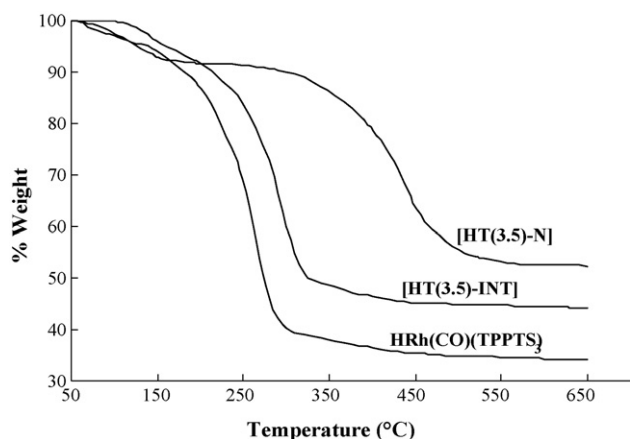
Fig. 4. TGA of HRh(CO)(TPPTS)$_3$ complex, [HT(3.5)-N] and [HT(3.5)-INT] catalysts.

alyst. Shifting of these bands in the direction of low frequency region is due to the coordination between oxygen atom of sulfonate group of HRh(CO)(TPPTS)$_3$ complex with the layers of hydroxide in the hydrotalcite network. Intensity of the band at 1381 cm^{-1} was observed to decrease significantly in the FT-IR spectrum of [HT(3.5)-INT] catalyst, which confirmed that the most of nitrate anions present in the interlayer space of hydrotalcite were replaced by HRh(CO)(TPPTS)$_3$ complex. Qualitative and quantitative analyses of the filtrate also confirmed the presence of a water soluble NaNO$_3$ salt. The other observed vibrations in the FT-IR spectra of HRh(CO)(TPPTS)$_3$ complex and [HT(3.5)-N] were found to be present in the FT-IR spectrum of [HT(3.5)-INT] catalyst. Above data show that the HRh(CO)(TPPTS)$_3$ complex is intercalated into interlayer space of [HT(3.5)-N].

^{31}P MAS NMR spectra of TPPTS, HRh(CO)(TPPTS)$_3$ complex and [HT(3.5)-INT] catalyst are shown in Fig. 3. The ^{31}P NMR spectra of TPPTS shows peaks at–5.4 and 34.65 ppm which is attributed to the uncoordinated TPPTS and oxides of TPPTS, respectively. The appearance of doublet at 44.32 [J(Rh–P) = 152 Hz] in ^{31}P NMR spectra of HRh(CO)(TPPTS)$_3$ complex shows the trigonal bipyramidal structure with three phosphorous atoms present in the same environment and are in equatorial plane. The hydride (H) and CO are in axial positions [40]. Doublet at 42.34 ppm was observed in solid state ^{31}P NMR spectra of [HT(3.5)-INT] catalyst, confirming that the HRh(CO)(TPPTS)$_3$ complex was intercalated into the interlayer space of the hydrotalcite. The observed doublet at 37.59 and sin-

glets at −31.48 ppm in solid state ^{31}P NMR spectra of [HT(3.5)-INT] catalyst are attributed to the intercalated HRh(CO)(TPPTS)$_2$ (which is an active species for hydroformylation of alkene) and TPPTS (intercalated), respectively in the interlayer space of hydrotalcite. During the intercalation process, dissociation of the TPPTS molecule from HRh(CO)(TPPTS)$_3$ complex was reported in the literature also [40,47,48]. The peak of OTPPTS (oxide of TPPTS) was observed at 34.65 ppm in the ^{31}P NMR spectrum of TPPTS (Fig. 3), however, no peak was observed at 34.65 ppm in the ^{31}P solid state NMR spectrum of [HT(3.5)-INT]. ^{31}P MAS NMR spectra of [HT(3.5)-INT] showed a peak at 8.37 ppm which could not be identified.

Thermal stability of HRh(CO)(TPPTS)$_3$, [HT(3.5)-N] and [HT(3.5)-INT] samples were evaluated by TGA and results are shown in Fig. 4. TGA of HRh(CO)(TPPTS)$_3$ showed 63% weight loss in the temperature range of 160–300 °C due to thermal decomposition of complex. However, only 3% weight loss of HRh(CO)(TPPTS)$_3$ was observed up to 140 °C due to the removal of water molecules. TGA of [HT(3.5)-N] showed weight loss in two stages, which is a typical characteristic of pure hydrotalcite sample [15]. The weight loss in first stage (9%) was observed in the temperature range of 200 °C due to loss of physically adsorb water molecules on the surface without collapse of the structure. The weight loss in second stage (30%) is attributed to the removal of hydroxyl groups and nitrate anions in the temperature range of 300–550 °C. TGA curve of [HT((3.5)-INT] catalyst was observed similar to the HRh(CO)(TPPTS)$_3$ complex. TGA of intercalated catalyst [HT((3.5)-INT] catalyst showed 10% weight loss in the temperature range of 140–200 °C due to removal of water molecules. The major weight loss (42%) was observed in second stage due to removal of anions from the interlayer space of hydrotalcite in the temperature range of 220–350 °C. The higher weight loss in [HT((3.5)-INT] as compared to pristine [HT((3.5)-N] is attributed to the decomposition of bulkier anions (TPPTS) from the interlayer space of [HT((3.5)-INT]. The observed higher thermal stability of [HT((3.5)-INT] catalyst as compared to HRh(CO)(TPPTS)$_3$ complex is due to the strong interaction of HRh(CO)(TPPTS)$_3$ complex and interlayer network of hydrotalcite structure. Due to the higher thermal stability of [HT((3.5)-INT], it has potential for catalytic applications in heterogeneous hydroformylation and hydrogenation reaction.

The SEM images of [HT(3.5)-N] and [HT(3.5)-INT] are given in Fig. 5. The micrographs of [HT(3.5)-N] and [HT(3.5)-INT] show a well developed layered structure and possess platelet structures. However, due to overlapping of such platelets spongy type structure is exhibited.
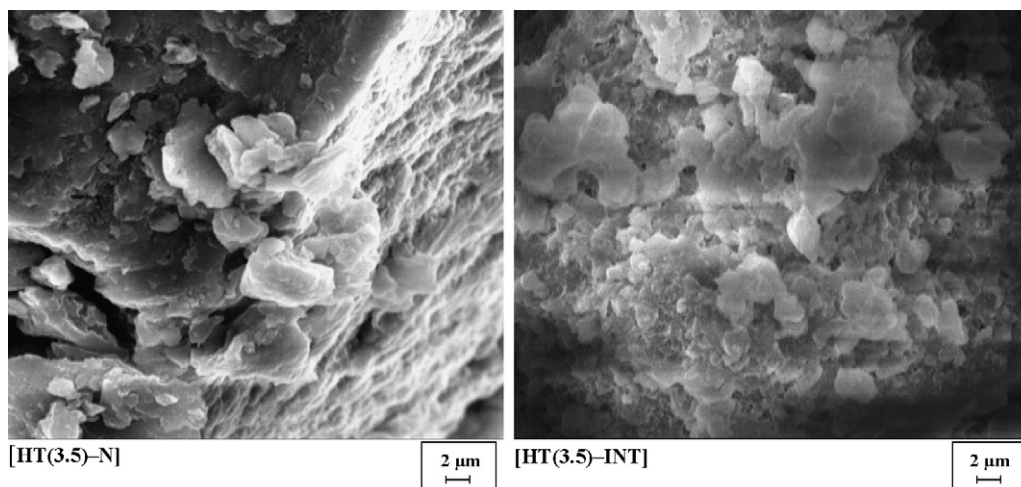

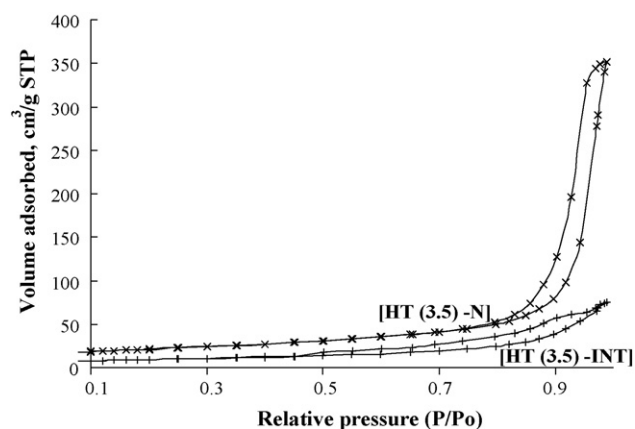**Fig. 5.** SEM images of [HT(3.5)-N] and [HT(3.5)-INT] catalysts.

Fig. 6. Surface area measurements of [HT(3.5)-N] and [HT(3.5)-INT] catalysts.

Nitrogen adsorption–desorption isotherms of [HT(3.5)-N] and [HT(3.5)-INT] samples measured at liquid nitrogen temperature are shown in Fig. 6. Surface area and pore volume of [HT(3.5)-N] and [HT(3.5)-INT] samples are given in Table 1. Surface area of [HT(3.5)-N] sample was calculated as 76 m^2/g that decreased up to 33 m^2/g after intercalation of HRh(CO)(TPPTS)$_3$ in interlayer space of [HT(3.5)-N]. Pore volume of [HT(3.5)-N] sample was also observed to decrease from 0.4 to 0.1 cm^3/g for intercalated [HT(3.5)-INT] catalyst. Surface area measurements data also support the results observed in P-XRD analysis of [HT(3.5)-INT] catalyst.

3.2. Catalytic activity for hydroformylation of alkenes

Catalytic activity of intercalated [HT(3.5)-INT] catalyst was evaluated for hydroformylation of linear alkenes with varied carbon number from C$_5$ to C$_{13}$ and some cyclic alkenes (Table 2). The mass fragmentation data of the products of hydroformylation of studied alkenes are given in Fig. 1 as the supporting materials file. As the carbon chain length of linear alkenes increases, the selectivity for aldehydes was observed to decrease. For example, 100% conversion with 98% selectivity of aldehydes was achieved for hydroformylation of 1-pentene in 10 h reaction time at 80 °C, which decreased to 99% conversion of 1-decene with 83% selectivity of aldehydes. However, for hydroformylation of 1-tridecene, conversion was further decreased to 88% with 56% selectivity of aldehydes. This decrease in the selectivity of aldehydes on increasing the carbon chain length of alkenes is due to faster isomerization of alkenes as compared to hydroformylation and formation of ketone under studied experimental conditions. Reactivity of the catalyst for hydroformylation of linear alkenes under identical reaction conditions was found to be in the order of; 1-pentene > 1-hexene > 1-heptene > 1-octene > 1-nonene > 1-decene > 1-undecene > 1-dodecene > 1-tridecene. The n/iso ratio of aldehydes for linear alkenes was observed in the range of 0.6–1.3. The main reason for lower n/iso ratio of aldehydes in the present study could be due to strong coordination of ligand to the hydrotalcite matrix in [HT(3.5)-INT] catalyst. Therefore, ligands

Table 1
Characterization of [HT(3.5)-N] and [HT(3.5)-INT] catalysts.

Sample	[HT(3.5)-N]	[HT(3.5)-INT]
Crystallinity, %	100	43
Surface area, m^2/g	76	33
Pore volume, cm^3/g	0.4	0.1
Unit cell parameter (a), Å	3.0	3.0
Unit cell parameter (c), Å	26.4	59.4
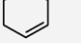
movement is restricted in intercalated catalyst as compared to that in its biphasic analogues [HRh(CO)(TPPTS)$_3$ catalyzed hydroformylation in biphasic medium], as a result, the steric effect of ligand is less operative to increase the n/iso ratio of aldehydes in this study. Another reason for lower n/iso ratio of aldehydes is due to the absence of excess ligand (TPPTS) in the present study. As to achieve higher n/iso ratio of aldehydes, isomerization of alkenes is normally suppressed by adding excess amount of ligand which creates a sterically demanding environment around the rhodium metal centre. Lower n/iso ratio of aldehydes in the range of 0.5–0.64 was also reported by the Chaudhary et al. for hydroformylation of alkenes using HRh(CO)(TPPTS)$_3$ supported on carbon surface [49].

In case of hydroformylation of cyclic alkenes, 98% conversion of cyclohexene with 100% selectivity for cyclohexanal (m/z = 112) was observed. The conversion decreased to 42% for cis–cyclooctene hydroformylation with 95% selectivity for cyclooctanal (m/z = 140). However, for the hydroformylation of 1-cycloheptene, 98% selectivity for cycloheptanemethanol (m/z = 128) was observed, which was formed via subsequently hydrogenation of hydroformylation product. The order of catalytic activity for the hydroformylation of cyclic alkenes was observed as; cyclohexene > cycloheptene > cyclooctene under identical reaction conditions. For hydroformylation of styrene, 95% conversion with 92% selectivity of aldehydes (3-phenylpropanal, α-phenylpropionaldehyde; m/z = 134) was observed, while the conversion decreased to 64% with 89% selectivity of aldehydes (benzenebutanal, α-ethyl-benzeneacetaldehyde; m/z = 148) for the hydroformylation of allylbenzene. The results described in Table 2 indicate that the HRhCO(TPPTS)$_3$ complex intercalated in hy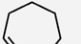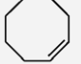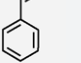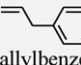drotalcite [HT(3.5)-INT] is an active heterogeneous catalyst for hydroformylation of various alkenes starting from n-alkenes (linear), cyclic as well as functionalized alkenes. In all the reactions, comparable catalytic activity was observed with its homogeneous analogues. 1-Hexene was selected as a model reactant to study the effect of reaction parameters such as, alkene concentration, amount of catalyst, partial pressure of CO and H$_2$ and reaction temperature on the catalytic activity of intercalated catalyst. The reusability of catalyst was also evaluated by performing repeated experiments under reaction conditions to those used for fresh catalyst.

3.3. Effect of 1–hexene concentration and amount of catalyst

Data on the conversion and selectivity for 1-hexene hydroformylation depicting the effect of varied concentration of 1-hexene and amount of catalyst are given in Table 3. 1-Hexene concentration was varied from 6 to 70 mmol keeping constant amount of the catalyst (100 mg). Complete conversion of 1-hexene was observed in the entire studied concentration range of 1-hexene. The selectivity of aldehydes was observed to increase up to 25 mmol concentration of 1-hexene. On further increasing the concentration of 1-hexene, the selectivity of aldehydes was found to decrease significantly. For example, selectivity of aldehydes increased from 74 to 95% on increasing the concentration of 1-hexene from 6 to 25 mmol and selectivity decreased to 83% on further increasing the concentration of 1-hexene to 50 mmol. The n/iso ratio of aldehydes was observed in the range of 0.6–0.8. The higher catalytic activity for isomerization of 1-hexene to 2/3-hexene at higher and lower substrate concentration results into the lower selectivity of aldehydes. Hydrogenation of 1-hexene and aldehydes was not observed in the present study. The calculated TOF values were found to increase from 52 to 648 on increasing the 1-hexene concentration from 6 to 70 mmol. The maximum conversion of 1-hexene and selectivity for aldehydes (n to iso ratio = 0.8) were observed at 25 mmol of 1-hexene concentration. Therefore,

Table 2
Effect of carbon number (chain length) of alkenes on catalytic activity of [HT(3.5)-INT][a].

Entry	Alkene	% Conversion	% Selectivity Aldehydes	n/iso ratio of aldehydes	Isomerization of alkene	Hydrogenation of alkene	Ketone
1	1–Pentene	100	98	1.3	2	–	–
2	1–Hexene	100	96	0.8	4	–	–
3	1–Heptene	100	95	0.8	5	–	–
4	1–Octene	100	95	0.7	5	–	–
5[b]	1–Nonene	100	88	0.7	7	–	5
6[c]	1–Decene	99	83	0.7	11	–	6
7[d]	1–Undecene	97	72	0.6	18	–	10
8[e]	1–Dodecene	95	67	0.6	21	–	12
9[f]	1–Tridecene	88	56	0.6	29	–	15
10	Cyclohexene	98	100	–	–	–	–
11[g]	Cycloheptene	90	–	–	–	2	–
12	cis–Cyclooctene	42	95	–	–	5	–
13	Styrene	95	92	0.5	–	8	–
14	allylbenzene	64	89	1.1	6	5	–

[a] Reaction conditions: alkene = 0.2 mmol, catalyst = 100 mg, syn-gas = 40 atm (CO/H_2 = 1/1), temperature = 80 °C, time = 10 h.
[b] 3-Decanone (m/z = 156).
[c] Undecanone.
[d] 3-Dodecanone (m/z = 184).
[e] Tridecanone (m/z = 198).
[f] 2-Tetradecanone (m/z = 212).
[g] 98% selectivity for cycloheptanemethanol (m/z = 128).

25 mmol concentration of 1-hexene was taken to study the effect of other reaction parameters on the conversion and selectivity for 1-hexene hydroformylation.

Effect of the amount of catalyst on the conversion and selectivity for 1-hexene hydroformylation was studied by varying the amount of catalyst from 10 to 500 mg at constant 1-hexene concentration (25 mmol). The selectivity of aldehydes was observed to increase up to 200 mg catalyst. On further increase in the amount of catalyst, the selectivity of aldehydes was observed to decrease significantly due to the higher selectivity of the 1-hexene isomerization products. The TOF values were expectedly observed to decrease on increasing the amount of catalyst. TOF value was calculated as 1014 at 10 mg catalyst amount, which decreased to 47 at 500 mg of catalyst amount.

3.4. Effect of partial pressure of H_2 and CO

Partial pressures of H_2 and CO have significant effect on the selectivity of aldehydes (Table 4). The effect of partial pressure of H_2 was studied by varying the pressure of H_2 from 2 to 30 atm at constant pressure of CO (20 atm). The conversion of 1-hexene was found to increase from 96 to 100% by increasing the partial pressure of H_2 from 2 to 10 atm. At lower partial pressure of H_2, lower selectivity of aldehydes was observed due to the slow hydroformylation of 1-hexene as compared to its isomerization. The selectivity of aldehydes was observed to increase significantly up to 20 atm, however, on further increase in partial pressure of H_2, no significant effect was observed. The selectivity of aldehydes was found to increase from 26 to 95% by increasing the pressure of H_2 from 2 to

Table 3
Effect of 1-hexene and catalyst amount on selectivity of aldehydes[a].

Entry	1-Hexene, mmol	Catalyst, mg	% Conversion	% Selectivity Aldehydes	n/iso ratio of aldehydes	2/3-Hexene	TOF, h^{-1}
1	6	100	100	74	0.6	26	52
2	12	100	100	89	0.7	11	125
3	18	100	100	94	0.7	6	198
4	25	100	100	95	0.8	5	281
5	30	100	100	92	0.8	8	323
6	40	100	100	89	0.7	11	375
7	50	100	100	83	0.7	17	466
8	70	100	100	77	0.7	23	648
9	25	10	91	35	0.9	65	1014
10	25	20	93	54	0.8	46	798
11	25	50	100	79	0.9	21	383
12	25	200	100	96	0.8	4	142
13	25	300	100	92	0.8	8	91
14	25	500	100	78	0.8	22	47

[a] Reaction conditions: syn-gas = 40 atm (CO/H$_2$ = 1/1), temperature = 80 °C, time = 8 h.

20 atm. The lower selectivity of aldehyde at lower partial pressure of hydrogen may be attributed to the insufficient concentration of hydrogen in the reaction medium. The selectivity of isomerization products (2/3-hexene) was observed to decrease from 74 to 4% on increasing the partial pressure of H$_2$ from 2 to 30 atm. The n/iso ratio of aldehydes was observed in the range of 0.7–0.9 on increasing the partial pressure of hydrogen from 2 to 30 atm. Higher value of the n/iso ratio of aldehydes at 30 atm hydrogen pressure could be attributed to the formation of HRh(CO)(TPPTS)$_2$ species, which favored the formation of linear aldehydes. The TOF was calculated as 75 at 2 atm and it increased to 287 at 30 atm partial pressure of hydrogen. Hydrogenation products of 1-hexene and aldehydes were not obtained under the studied reaction conditions or even at 30 atm partial pressure of H$_2$. Effect of the partial pressure of CO on conversion and selectivity was also studied at constant H$_2$ pressure (20 atm). The selectivity for aldehydes was observed to increase from 47% at 5 atm to 98% at 30 atm of CO partial pressure. The selectivity of 2/3-hexene decreased significantly from 53 to 8% by increasing the partial pressure of CO from 5 to 15 atm and selectivity of 2/3-hexene again decreased to 2% on further increasing the partial pressure of CO to 30 atm. The TOF values were observed

to increase from 135 to 290 on increasing the partial pressure of CO from 5 to 30 atm. The reason for lower selectivity of aldehydes at lower partial pressure of CO is the insufficient concentration of CO to forward the hydroformylation reaction. As partial pressure of CO increased, the selectivity of aldehydes was observed to increase due to the enhancement in the CO concentration.

3.5. Effect of reaction temperature

The reaction temperature was varied from 50 to 100 °C at 40 atm pressure of syn-gas (CO/H$_2$ = 1), 100 mg catalyst and 0.025 mol of 1-hexene concentration (Table 5). The selectivity of aldehydes was observed to increase from 78 to 95% on increasing the reaction temperature from 50 to 80 °C. On further increase in the reaction temperature to 100 °C, the selectivity for aldehydes decreased to 53%. The observed decrease in the aldehydes selectivity is due to the increased isomerization of 1-hexene to 2/3-hexene at higher reaction temperature. At 80 °C, 5% isomerization of 1-hexene was obtained and it increased to 47% at 100 °C. The n/iso ratio of aldehydes was also found in the range of 1.1–0.8 on increasing the reaction temperature from 50 to 100 °C. At higher temperatures,

Table 4
Effect of partial pressure of H$_2$ and CO on selectivity of aldehydes[a].

Entry	Partial pressure of H$_2$, atm	CO, atm	% Conversion	% Selectivity Aldehydes	n/iso ratio of aldehydes	2/3–Hexene	TOF, h^{-1}
1	2	20	96	26	0.7	74	75
2	10	20	100	50	0.7	50	148
3	15	20	100	89	0.7	11	263
4	20	20	100	95	0.8	5	281
5	30	20	100	96	0.9	4	287
6	20	5	97	47	0.7	53	135
7	20	10	100	78	0.7	22	231
8	20	15	100	92	0.7	8	272
9	20	20	100	95	0.8	5	281
10	20	30	100	98	0.8	2	290

[a] Reaction conditions: 1-hexene = 25 mmol, catalyst = 100 mg, temperature = 80 °C time = 8 h.

Table 5
Effect of temperature on selectivity of aldehydes[a].

Entry	Temperature °C	% Conversion	% Selectivity Aldehydes	n/iso ratio of aldehydes	2/3-Hexene	TOF, h^{-1}
1	50	100	78	1.1	22	230
2	60	100	89	0.9	11	263
3	70	100	93	0.9	7	275
4	80	100	95	0.8	5	281
5	100	100	53	0.8	47	157

[a] Reaction conditions: 1-hexene = 25 mmol, catalyst = 100 mg, syn-gas = 40 atm (CO/H$_2$ = 1/1) time = 8 h.

Table 6
Catalytic activity of [HT(3.5)-INT] with its counterpart HRh(CO)(TPPTS)$_3$ in biphasic system and other supported catalysts for hydroformylation of 1-hexene.

Catalyst	% Conversion	% Selectivity of aldehyde	n/iso ratio	TOF (h^{-1})	Ref.
HRh(CO)(TPPTS)$_3$ intercalated in HT	100	74–95	0.6–0.9	52–1014	Present study
HRh(CO)(TPPTS)$_3$	100	100	1.5	810	[52]
RhCl(CO)(TPPTS)$_2$ intercalated in Zn$_2$-Al LDH with excess TPPTS	75.94	84.34	2.19	266.97	[53]
RhCl(CO)(TPPTS)$_2$ intercalated in Zn$_3$-Al LDH with excess TPPTS	60–95	70–80	2.6–3.0	80–150	[38]
Rh/SiO$_2$	93.6	5.82	1.7	11.7	[48]
TPPTS-Rh/SiO$_2$	23.8	92.4	6.1	51.7	[48]
RhH(CO)(TPPTS)$_3$ supported on SiO$_2$-FA	72.9	75	3.2	454.2	[54]

it is expected that the thermal motion of intermediate catalytic species increases due to significant decrease in steric factors of the catalyst which results into increase in polarity of M–H bond favoring Markovnikov addition that results into higher selectivity of *iso*-aldehyde. Another reason for the lower *n/iso* ratio of aldehydes at higher temperature could be attributed to the higher concentration of the intercalated HRh(CO)$_2$(TPPTS)$_2$ species, which are responsible for the formation of branched aldehydes. Calculated TOF values were observed to increase up to 80 °C and decreased on further increase in the reaction temperature.

3.6. Kinetics measurements and reusability of the catalyst

The reaction profile with respect to time for hydroformylation of 1-hexene using [HT(3.5)-INT] catalyst at 80 °C and 40 atm syngas pressure is shown in Fig. 7. Rapid consumption of 1-hexene was observed for hydroformylation and isomerization reactions. Initially, most of 1-hexene isomerized to 2/3-hexene in the studied experimental conditions. About 95% conversion of 1-hexene into 2/3-hexene was observed within 60 min reaction time. However, after complete consumption of 1-hexene, 2/3-hexene was converted into aldehydes (mostly for 2-methylhexanal and 2-ethylpentanal) via hydroformylation reaction which results into lower *n/iso* ratio of aldehydes. Higher rate of reaction was obtained for isomerization of 1-hexene to 2/3-hexene as compared to the hydroformylation reaction. The higher rate of isomerization reaction is due to the well known property of the Rh-complex and hydrotalcite for double bond isomerization [50,51]. Hydrogenation products were not observed during the course of kinetics experiment.

The catalyst was re-cycled up to seven times for hydroformylation of 1-hexene (Fig. 8). Complete conversion of 1-hexene (100%) was observed in seventh cycle, however, selectivity of the aldehydes (*n* and *iso*) was observed to decrease after fifth cycle. The 93% selectivity of aldehydes was obtained at fifth cycle that decreased to 87% at the end of seventh cycle. The decrease in selectivity of alde-
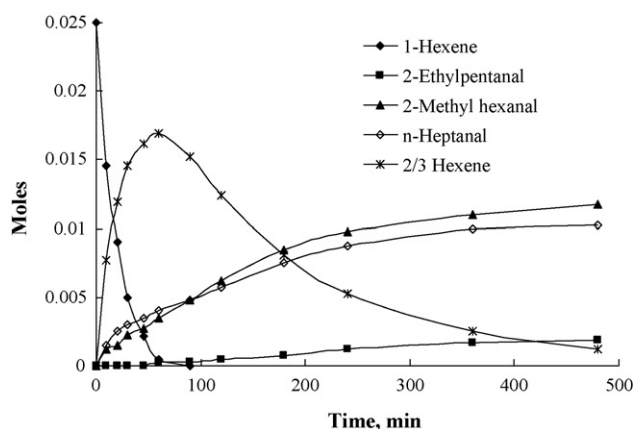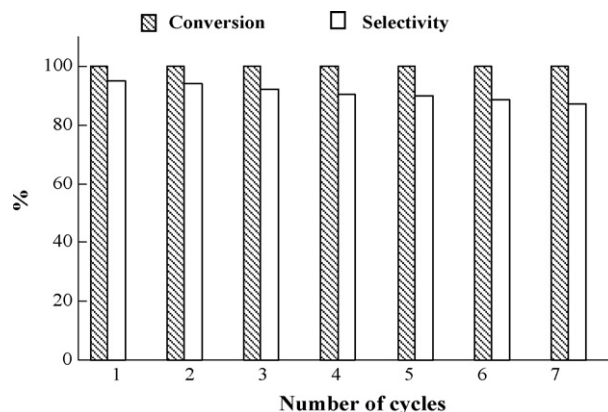

Fig. 8. Reusability of [HT(3.5)-INT] catalyst for hydroformylation of 1-hexene.

hydes could be ascribed to handling losses of the catalyst (since catalyst is air sensitive) and leaching of rhodium (1.5% (by wt) leached out after seventh cycle as compared to initial amount) during reusability experiments. However, leaching of rhodium from [HT(3.5)-INT] catalyst is lower in the present study as compared to other reported heterogeneous catalyst [38]. The P-XRD and FT-IR spectrum of used [HT(3.5)-INT] catalyst shown in Figs. 1 and 2 also supported that the structure of [HT(3.5)-INT] catalyst was not disturbed significantly after repeated experiments with the same catalyst.

The catalytic activity of [HT(3.5)-INT] was compared with its counterpart HRh(CO)(TPPTS)$_3$ in biphasic system and other supported catalysts for hydroformylation of 1-hexene (Table 6). The HRh(CO)(TPPTS)$_3$ catalyst in biphasic system gave 100% conversion with 100% selectivity of aldehyde, however, the catalyst is re-cycled up to three cycles [52]. After third cycle significant drop in the conversion of 1-hexene is reported. The catalyst reported in the present study showed higher conversion of 1-hexene and higher selectivity of aldehydes with lower *n/iso* ratio as compared to other HRh(CO)(TPPTS)$_3$ supported catalysts reported in the literature [38,52–54].

4. Conclusions

Intercalation of HRh(CO)(TPPTS)$_3$ complex into interlayer space of hydrotalcite was confirmed by ^{31}P NMR, P-XRD and FT-IR spectra of intercalated [HT(3.5)-INT] catalyst. Catalytic activity of intercalated catalyst was evaluated for hydroformylation of linear alkenes with varied carbon number (C$_5$–C$_{13}$) and cyclic alkenes. As carbon chain length of linear alkenes increases, the selectivity of aldehydes was observed to decrease. Activity of the catalyst for hydroformylation of linear alkenes under identical reaction conditions was found to be in the order of; 1-pentene > 1-hexene > 1-heptene > 1-octene > 1-nonene > 1-decene > 1-undecene > 1-dodecene > 1-tridecene. Order of the catalytic activity for hydroformylation of cyclic alkenes was observed as; cyclohexene > cycloheptene > cyclooctene under

Fig. 7. Kinetic profile for hydroformylation of 1-hexene using [HT(3.5)-INT] as a catalyst.

identical reaction conditions. The catalyst was re-cycled up to five times without significant loss in conversion and selectivity for hydroformylation of 1-hexene.

Acknowledgements

References

[1] C.D. Frohning, C.W. Kohlpaintner, B. Cornils, W.A. Hermann, Applied Homogeneous Catalysis with Organometallic Compounds, Wiley–VCH, Weinheim, 2000, p. 29.
[2] V.K. Srivastava, D.U. Parmar, R.V. Jasra, Chem. Weekly (2003) 173–178.
[3] Chemical Economic Handbook, Oxo Chemical Report, SRI International, January 2003.
[4] E.G. Kunzu, FR 2 349 562; 2 366 237; 2 733 516 (1976) to Rhone–Poulenc.
[5] K. Mukhopadhyay, R.V. Chaudhari, J. Catal. 213 (2003) 73–77.
[6] L. Huang, Y. He, S. Kawi, J. Mol. Catal. A: Chem. 213 (2004) 241–249.
[7] L. Huang, S. Kawi, Catal. Lett. 92 (2004) 57–62.
[8] R.J. Davis, J.A. Rossin, M.E. Davis, J. Catal. 98 (1986) 477–486.
[9] M.W. Balakos, S.S.C. Chuang, J. Catal. 151 (1995) 266–278.
[10] A. Riisager, P. Wasserscheid, R. Hal, R. Fehrmann, J. Catal. 219 (2003) 452–455.
[11] H. Arai, J. Catal. 51 (1978) 135–142.
[12] K. Mukhopadhyay, A.B. Mandale, R.V. Chaudhari, Chem. Mater. 15 (2003) 1766–1777.
[13] M. Ichikawa, J. Catal. 59 (1979) 67–78.
[14] (a) Y. Zhang, K. Nagasaka, X. Qiu, N. Tsubaki, Appl. Catal. A: Gen. 276 (2004) 103–111;
(b) I.T. Horvath, J. Rabai, Science 266 (1994) 72;
D.F. Foster, D. Gudmunsen, D.J. Adams, A.M. Stuart, E.G. Hope, D.J. Cole-Hamilton, G.P. Schwarz, P. Pogorzelec, Tetrahedron 58 (2002) 3901–3910;
Liu and Xiao, 2007 S. Liu, J. Xiao, J. Mol. Catal. A: Chem. 270 (2007) 1–43.
[15] F. Cavani, F. Trifiro, A. Vaccari, Catal. Today 11 (1991) 173–301.
[16] D.G. Evans, X. Duan, Chem. Commun. (2006) 485–496.
[17] A.I. Khan, D. O'Hare, J. Mater. Chem. 12 (2002) 3191–3198.
[18] E.L. Crepaldi, P.C. Pavan, J.B. Valim, Chem. Commun. (1999) 155–156.
[19] R. Schollhorn, B. Otto, J. Chem. Soc., Chem. Commun. (1986) 1222–1223.
[20] K. Chibwe, W. Jones, J. Chem. Soc., Chem. Commun. 14 (1989) 926–927.
[21] A.I. Khan, L. Lei, A.J. Norquist, D. O'Hare, Chem. Commun. 22 (2001) 2342–2343.
[22] G.R. Williams, T.G. Dunbar, A.J. Beer, A.M. Fogg, D. O'Hare, J. Mater. Chem. 13 (2006) 1231–1237.
[23] K.M. Parida, S. Parija, J. Das, P.S. Mukherjee, Catal. Commun. 7 (2006) 913–919.
[24] J. Das, K.M. Parida, J. Mol. Catal. A: Chem. 264 (2007) 248–254.
[25] E. Kanezaki, K. Kinugawa, Y. Ishikawa, Chem. Phys. Lett. 226 (1994) 325–330.
[26] F. Malherbe, J.-P. Besse, J. Solid State Chem. 155 (2000) 332–341.
[27] E.L. Crepaldi, P.C. Pavan, J. Tronto, J.B. Valim, J. Colloid Interface Sci. 248 (2002) 429–442.
[28] V.I. Iliev, A.I. Ileva, L.D. Dimitrov, Appl. Catal. A: Gen. 126 (1995) 333–340.
[29] B.M. Choudary, M.L. Kantam, N.M. Reddy, N.M. Gupta, Catal. Lett. 82 (2002) 79–83.
[30] M. Chibwe, T.J. Pinnavaia, J. Chem. Soc., Chem. Commun. 3 (1993) 278–280.
[31] S. Hamada, K. Ikeue, M. Machida, Chem. Mater. 17 (2005) 4873–4879.
[32] J. Inacio, C.T. Gueho, S.M. Therias, M.E. Roy, J.P. Besse, J. Mater. Chem. 11 (2001) 640–643.
[33] E.P. Giannelis, D.G. Nocera, T.J. Pinnavaia, Inorg. Chem. 26 (1987) 203–205.
[34] I. Crespo, C. Barriga, V. Rives, M.A. Ulibarri, Solid State Ionics 101–103 (1997) 729–735.
[35] M. Arco, S. Gutierrez, C. Martin, V. Rives, Inorg. Chem. 42 (2003) 4232–4240.
[36] I. Carpani, M. Berrettoni, M. Giorgetti, D. Tonelli, J. Phys. Chem. B 110 (2006) 7265–7269.
[37] N.H. Gutmann, L. Spiccia, T.W. Turney, J. Mater. Chem. 10 (2000) 1219–1224.
[38] X. Zhang, M. Wei, M. Pu, X. Li, H. Chen, D.G. Evans, X. Duan, J. Solid State Chem 178 (2005) 2701–2708;
M. Wei, X. Zhang, D.G. Evans, X. Duan, X. Li, H. Chen, AIChE J. 53 (2007) 2916–2924.
[39] F. Iosif, V.I. Parvulescu, M.E. Perez-Bernal, R.J. Ruano-Casero, V. Rives, K. Kranjc, S. Polanc, M. Kocevar, E. Genin, J.-P. Genet, V. Michelet, J. Mol. Catal. A: Chem. 276 (2007) 34–70.
[40] J.P. Arhancet, M.E. Davis, J.S. Merola, B.E. Hanson, J. Catal. 121 (1990) 327.
[41] Y. Zhao, F. Li, R. Zhang, D.G. Evans, X. Duan, Chem. Mater. 14 (2002) 4286–4291.
[42] E.P. Barrett, L.G. Joyner, P.P. Halenda, J. Am. Chem. Soc. 73 (1951) 373–380.
[43] V.K. Srivastava, S.K. Sharma, R.S. Shukla, N. Subrahmanyam, R.V. Jasra, Ind. Eng. Chem. Res. 44 (2005) 1764–1771.
[44] V.K. Srivastava, R.S. Shukla, H.C. Bajaj, R.V. Jasra, Appl. Catal. A: Gen. 282 (2005) 31–38.
[45] S.K. Sharma, V.K. Srivastava, R.S. Shukla, P.A. Parikh, R.V. Jasra, New J. Chem. 31 (2007) 277–286.
[46] V.K. Srivastava, S.K. Sharma, R.S. Shukla, R.V. Jasra, Catal. Commun. 7 (2006) 881–886.
[47] C. Bianchini, H.M. Lee, A. Meli, F. Vizza, Organometallics 19 (2000) 849–853, and reference cited therein.
[48] H. Zhu, Y. Ding, H. Yin, L. Yan, J. Xiong, Y. Lu, H. Luo, L. Lin, Appl. Catal. A: Gen. 245 (2003) 111–117, and reference cited therein.
[49] N.S. Pagar, R.M. Deshpande, R.V. Chaudhari, Catal. Lett. 110 (2006) 129–133.
[50] V.K. Srivastava, H.C. Bajaj, R.V. Jasra, Catal. Commun. 4 (2003) 543–548.
[51] S.K. Sharma, V.K. Srivastava, P.H. Pandya, R.V. Jasra, Catal. Commun. 6 (2005) 205–209.
[52] P.J. Baricelli, E. Lujano, M. Modrono, A.C. Marrero, Y.M. Garcıa, A. Fuentes, R.A. Sanchez-Delgado, J. Organomet. Chem. 689 (2004) 3782–3792.
[53] Z. Xian, L. Jun, J. Lan, W. Min, Chin. Sci. Bull. 53 (2008) 1329–1336.
[54] Z. Li, Q. Peng, Y. Yuan, Appl. Catal. A: Gen. 239 (2003) 79–86.